 doi:10.20944/preprints202204.0223.v1

Article

Effect Of Sulfate Ions on Galvanized Post-Tensioned Steel Corrosion in Alkaline Solutions and the Interaction with Other Ions

Andrés Bonilla [1], Cristina Argiz [1],Amparo Moragues[1*], Jaime C. Gálvez[1].

[1] Departamento de Ingeniería Civil, Construcción, E.T.S de Ingenieros de Caminos, Canales y Puertos, Universidad Politécnica de Madrid, c/ Profesor Aranguren, s/n, 28040 Madrid, Spain; af.bonilla@alumnos.upm.es; cg.argiz @upm.es; amparo.moragues@upm.es; jaime.galvez@upm.es

* Correspondance : amparo.moragues@upm.es

Abstract: Zinc protection of galvanized steel is initially dissolved in alkaline solutions. However, passive layer is formed over time which protects the steel from corrosion. The behavior of galvanized steel exposed to strong alkaline solutions (pH values of 12.7) with a fixed concentration of sulfate ion of 0.04M is studied. Electrochemical measurement techniques such as corrosion potential, linear polarization resistance and electrochemical impedance spectroscopy are used. Synergistic effect of sulfate ion is also studied together with other anions such as chloride Cl^- or bicarbonate ion HCO_3^- and with other cations such as calcium Ca^{2+}, ammonium NH_4^+ and magnesium Mg^{2+}. Presence of sulfate ions can depassivate the steel, leading to corrosion density of 0.3 μA/cm² at the end of the test. The presence of other ions in the solution increases this effect. The increase in corrosion density caused by cations and anions responds to the following order (greater to lesser influence): $NH_4^+ > Ca^{2+} > Mg^{2+}$ and $HCO_3^- > Cl^- > SO_4^{2-}$.

Keywords: Corrosion; Sulfate; Galvanized Steel; Alkaline solutions; Linear Polarization Resistance; Electrochemical Impedance Spectroscopy

1. Introduction

Corrosion phenomenon usually causes more severe damage to prestressed steel structures than to conventional reinforced concrete structures. Protection of prestressed galvanized steel wires was ensured by injecting alkaline grout into polyethylene ducts covering the strands. However, in areas not protected by these ducts, in deteriorated places, or in areas with insufficient grout, corrosion phenomena can occur. Accumulation in these areas of contaminated water with aggressive ions coming from the atmosphere, marine environments or with decomposition products of organic matter can cause corrosion of these wires and failures in the post-tensioned strands.

Galvanizing protects steel through two mechanisms. Firstly, it creates a physical barrier that isolates it and acts as a sacrificial anode. In addition, corrosion products create a second protective barrier. Behavior of zinc in alkaline media has already been considered in the literature[1–3]. Zinc in contact with the alkaline matrix of cement in the fresh state shows temporary chemical instability. High pH values of the aqueous phase inside concrete pores, usually above 12.5, cause zinc oxidation. The cathodic reaction is associated with water hydrolysis and generates hydrogen on the galvanized surface, according to Equation (1).

$$2H_2O + 2e^- \longrightarrow 2OH^- + H_{2(g)} \quad (1)$$

Preprints (www.preprints.org) | NOT PEER-REVIEWED | Posted: 25 April 2022 doi:10.20944/preprints202204.0223.v1

The possible transformation of molecular hydrogen into physic-sorpbided atomic hydrogen, proposed by Riecke [4], increases the risk of hydrogen embrittlement in galvanized post-tensioned steel.

Pourbaix diagram of zinc indicates that, at pH value around 12, it forms insoluble oxides layer of ZnO/$Zn(OH)_2$ more stable than the oxide layer formed at pH 13. With high alkalinities, Zn has an amphoteric behavior forming soluble ions $Zn(OH)^{3-}$ and $Zn(OH)_4^{2-}$ [5]. Formation of $Zn(OH)_2$ leads to hydrogen formation [6]:

$$Zn + 2H_2O \rightarrow Zn(OH)_2 + H_{2(g)} \quad (2)$$

Risk of corrosion in an alkaline medium and in presence of calcium ions can be limited due to the formation of a passive layer of calcium hydroxyzincate $Ca(Zn(OH)_3)_2{\cdot}2H_2O$ stable and protective. Some authors [7,8], identify a value of pH 13.3 ± 0.1 as the limit for the passivation of galvanized steel. At a lower value of pH than 13.3, $Ca(Zn(OH)_3)_2{\cdot}2H_2O$ crystals are small enough to form a thin, homogeneous and stable layer on the surface of the steel capable of keeping it passive. At a higher value of pH than 13.3 and when the calcium content is low, the size of the crystals increases, making it difficult to cover the entire surface of the galvanized steel. In this case, large, isolated $Ca(Zn(OH)_3)_2$ crystals that do not passivate galvanized steel are formed.

Other works [9], studied the behavior of galvanized steel as function of pH in the absence of Ca^{2+} ions. Between 12 <pH <12.8 the galvanized layer dissolves at a slow speed. In the range of 12.8 <pH <13.3 the galvanized layer is capable of being covered with a protective layer that insulates it. Although at pH> 12.8 ± 0.1 hydrogen formation release occurs. At a value of pH> 13.3 the galvanizing layer dissolves completely. It is worth noting that the role of sulfate ion in the corrosion of galvanized steel has been less studied. Acha [10], studied stress corrosion of prestressed steel immersed in saturated solutions of $Ca(OH)_2$ with five concentrations of sulfate ions at various values of pH (0.01M SO_4^{2-} at a pH of 12.1; 0.025M SO_4^{2-} at a pH of 12.2; 0.05M SO_4^{2-} at a pH of 12.4; 0.1M and 0.2M SO_4^{2-} at a pH of 12.85). Results showed a limiting sulfate concentration between 0.025 (pH = 12.2) and 0.05 (pH = 12.4). Above this limit steel surface presented severe localized corrosion and below this concentration limit, steel remained passive. Liu et al.[11] also showed that a sulfate concentration between 0.02 and 0.03 mol/l, in a saturated solution of $Ca(OH)_2$, produced steel corrosion.

Therefore, corrosion of prestressed steel in presence of sulfates depends on the sulphate ion concentration in the solution and on the pH. Carsana and Bertolini [12] indicated a dependence of pH on the anodic behavior of steel in sulphate solutions for the corrosion of the steel. Acha's thesis also addressed the study of bicarbonate ion effect (0.05M concentration combined with pH = 11 and 0.1M concentration with pH = 8.2) and of carbonate ion (CO_3^{2-}) in saturated solutions of $Ca(OH)_2$. In both cases, current density reaches values lower than 0.2μA/cm2 after 45 days. These ions do not cause corrosion problems in prestressed steel.

In alkaline media and in presence of carbonates, most common corrosion product is hydrozincite ($Zn_5(CO_3)_2(OH)_6$) [13,14], and, in presence of sulfates zinc, hydroxysulfate ($Zn_4(SO_4)(OH)_6{\cdot}3H_2O$). After galvanized steel exposure to marine environments, formation of a passive layer of hexagonal crystals of simonkolleite $Zn_5Cl_2(OH)_8{\cdot}H_2O$, and zincite ZnO, is identified as the main corrosion product. Simonkolleite is formed after hydrozincite, both being white crystalline compounds. Later, a more protective layer of gordaite $NaZn_4Cl(OH)_6SO_4{\cdot}6H_2O$ can be formed by incorporation of sulfate and sodium ions in the crystalline structure of simonkolleite. Soluble compounds such as $ZnCl_2$ and $ZnSO_4$ have also been identified in marine environments[13,15–19].

Xu et al [20], studied the effect of the cation coming from different sulfate salts ($MgSO_4$, $(NH_4)_2SO_4$, Na_2SO_4, $CaSO_4$) added in a fixed concentration of 0.01mol/l. Corrosion study was made in saturated calcium hydroxide solutions. Solutions of magnesium sulfate and ammonium sulfate show higher rates of corrosion than solution with sodium

 doi:10.20944/preprints202204.0223.v1

sulfate. Solution pH is lowered with addition of ammonium sulfate and magnesium sulfate. Neupane *et al.* [21] studied NH^{4+}, Na^{+}, and Mg^{2+} cations effect on corrosion of galvanized steel. Solutions of $(NH_4)_2SO_4$, Na_2SO_4 and $MgSO_4$ 0.5M were prepared in distilled water. The increase in corrosion density caused by cations and anions responds to the following order (greater to lesser influence): Na^{+}>NH_4^{+}>Mg^{2+}. Magnesium ion forms finer, more compact and less porous corrosion products than the other salts.

There are numerous studies on the influence of potentially aggressive ions on the corrosion of galvanized steel. The results obtained show that the critical concentrations for each ion are often determined by the pH value of the solution. However, the effect that the joint presence of two or more potentially aggressive ions generates has not been determined. In the present work is studied the effect of sulfate ion in alkaline solution and the synergistic effect of various cations and anions found in seawater or marine environments (Ca^{2+}, NH_4^{+}, HCO^{3-}, Mg^{2+} and Cl^{-}) or in the atmosphere of corroding galvanized steel wires.

2. Experimental Work

2.1 Solutions

Concentrations of different ions have been used based on those obtained in real solutions, obtained by action of rainwater with degradation processes of living beings waste. Table 1 indicates ionic composition of six synthetic solutions prepared from the following salts: Na_2SO_4, $Ca(OH)_2$, NH_4COOH, $NaHCO_3$, $Mg(COOH)_2$ and NaCl. Solutions pH was set at 12.7 by adjusting with NaOH 2M. The main component was sulfate ion, followed by magnesium, chloride and ammonium. Ions were introduced incrementally in order to determine which ones were responsible for corrosion initiation.

Table 1. Composition of synthetic solutions prepared for corrosion tests.

Solution	SO_4^{2-} [mol/l] 0.04	Ca^{2+} [mol/l] $4{\cdot}10^{-4}$	NH_4^{+} [mol/l] $5{\cdot}10^{-3}$	HCO^{3-} [mol/l] $4{\cdot}10^{-4}$	Mg^{2+} [mol/l] $9.6{\cdot}10^{-3}$	Cl^{-} [mol/l] $7.6{\cdot}10^{-3}$
1	X					
2	X	X				
3	X	X	X			
4	X	X	X	X		
5	X	X	X	X	X	
6	X	X	X	X	X	X

2.2 Corrosion Electrochemical Cells

Electrochemical cells were made in polypropylene bottles with three-electrode system (Figure 1). An Ag/AgCl electrode was used as a reference electrode. Stainless steel mesh was used as a counter electrode and galvanized wire (nominal diameter of 0.519 cm) as a working electrode. Galvanized wires were cleaned with alcohol. Adhesive tape was used for limiting and exposed attack area of 4,891 cm^2. To avoid carbonation, the solution was covered with a liquid paraffin layer.

Preprints (www.preprints.org) | NOT PEER-REVIEWED | Posted: 25 April 2022 doi:10.20944/preprints202204.0223.v1

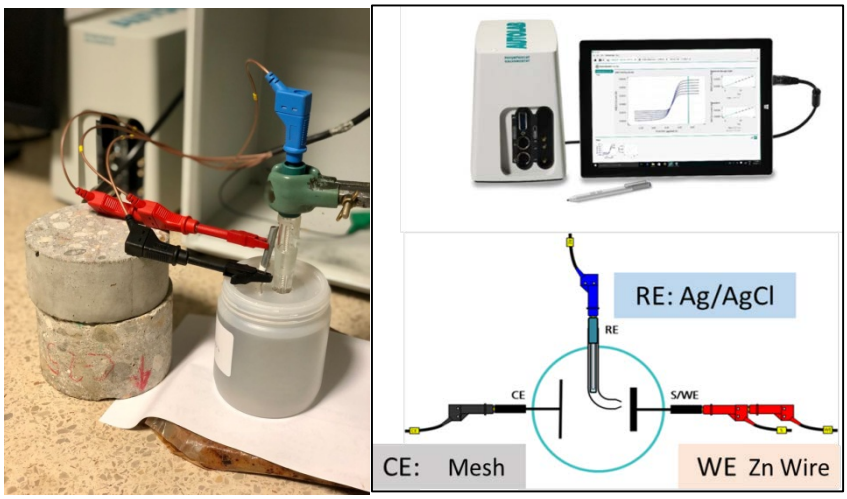

Figure 1. Corrosion cell and Autolab PGSTAT 204 potentiostat/galvanostat assembly together with experimental connections.

2.3 Techniques

2.3.1. Electrochemical Tests

Electrochemical tests were carried out with Autolab PGSTAT 204 potentiostat/galvanostat from Metrohm Autolab BV®. NOVA 2.4.1 software with FRA 32 impedance module (Figure 1) was used. Linear polarization resistance (LPR) and electrochemical impedance spectroscopy (EIS) were also used. LPR method was used to determine the instantaneous corrosion rate [22, 23]. Measurement was carried out applying polarization scan from -20mV to 20mV around the open circuit potential (OCP) at a sweep rate of 0.1667 mV/s. Ohmic drop (R_Ω) obtained by electrochemical impedance technique is subtracted from this resistance. Therefore, charge transfer resistance between zinc surface and solution (R_p) (Equation 3) is calculated as:

$$R_p = R_{p\,(LPR)} - R_{\Omega\,(EIS)} \quad (3)$$

Corrosion density (I_{corr}) was achieve from the polarization resistance (R_p) calculated as the slope of the polarization curve around the corrosion potential according to the Stern and Geary relationship (Equation 4) (Stern, M; Geary, A, L., 1957) (with parameter B=13) [8, 24–26] and the procedure proposed in UNE 112072 standard [22].

$$I_{corr} = B \cdot \frac{1}{R_p \cdot A} \quad (4)$$

Impedance measurements (EIS) were performed by potentiostatic control in frequency range between 10mHz and 100Khz, taking 10 points per decade. Amplitude of the input AC voltage signal was ± 10 Mv (rms). This technique consists of making measurements through small signal of alternating current and constant voltage to a working electrode, making frequency sweeps of the applied signal [24, 25, 27].

2.3.2. Electron Microscopy SEM/EDS

At the end of the tests, steels were extracted from the solution, dried in an oven at 40°C for a week , and then the surface morphology was observed by using Electron Microscopy SEM/EDS. Attacked zone of the galvanized steel was observed by scanning electron microscope. A JEOL 6400 JSM microscope with EDS analysis was used with a resolution of 133 eV.

Preprints (www.preprints.org) | NOT PEER-REVIEWED | Posted: 25 April 2022 doi:10.20944/preprints202204.0223.v1

2.3.3. Optical Microscopy

In addition, an OLYMPUS SZX7 optical microscope with an OLYMPUS SC50 camera was used to characterize and observe wires surface after exposure to the corresponding solutions.

3. Results and Discussion

3.1. LPR Results

Figure 2 shows polarization curves resulting from the last LPR test. Curves show the cathodic and anodic branch, and corrosion potential. All zinc wires showed their potentials at intermediate corrosion probability (Ecorr > -332mV) except for solution 4 with somewhat higher values.

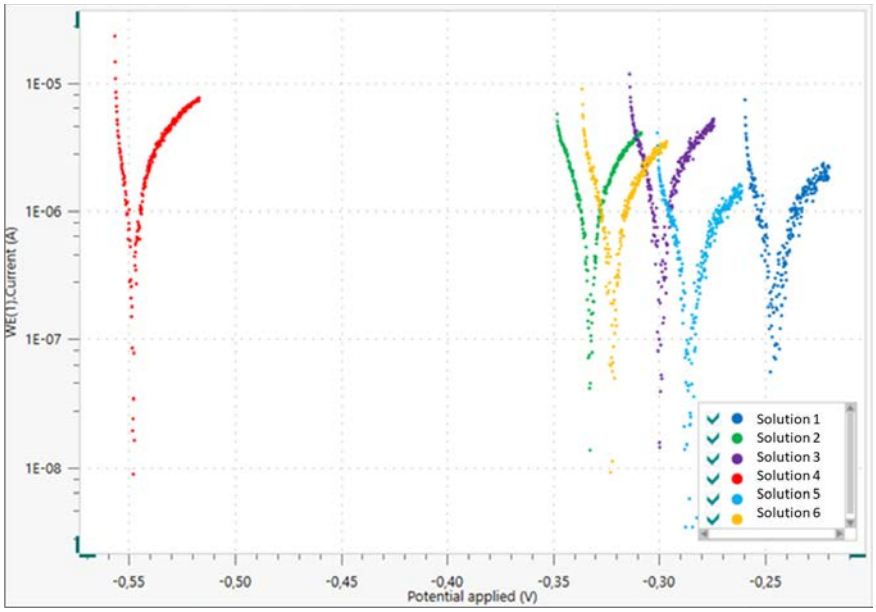

Figure 2. Polarization curves of zinc wires in solution cells after 35 days of manufacture.

Table 2 shows values obtained for E_{corr}, R_p and I_{corr} of all synthetic solutions made during the entire test period. Wires evolve from high corrosion risk to less electronegative potentials. Figure 3 shows evolution in time of I_{corr} and E_{corr} of the wires.

Table 2. Electrochemical parameters obtained after 35 days of manufacture.

Day	Solution 1			Solution 2			Solution 3		
	Ecorr (mV)	Rp (Ω)	Icorr (μA/cm²)	Ecorr (mV)	Rp (Ω)	Icorr (μA/cm²)	Ecorr (mV)	Rp (Ω)	Icorr (μA/cm²)
0	-1403	27.33	97.24	-1373	56.23	47.26	-1396	28.75	92.45
1	-1396	31.45	84.51	-1386	42.26	62.89	-1389	28.30	93.92
8	-1379	20.57	129.20	-1375	55.35	63.35	-1375	21.17	125.54
28	-261	7290.27	0.36	-1351	31.50	84.37	-	-	-
35	-246	9383.37	0.28	-332	5039.88	0.53	-300	4306.20	0.62

Day	Solution 4			Solution 5			Solution 6		
	Ecorr (mV)	Rp (Ω)	Icorr (μA/cm²)	Ecorr (mV)	Rp (Ω)	Icorr (μA/cm²)	Ecorr (mV)	Rp (Ω)	Icorr (μA/cm²)
0	-1387	36.67	72.48	-1384	26.07	101.94	-1393	22.43	118.51

Preprints (www.preprints.org) | NOT PEER-REVIEWED | Posted: 25 April 2022 doi:10.20944/preprints202204.0223.v1

1	-1382	25.64	103.66	-1385	25.42	104.54	-1389	28.15	94.40
8	-1367	32.10	82.79	-1379	26.97	98.54	-1378	32.95	80.66
28	-593	2595.41	1.02	-	-	-	-	-	-
35	-548	3660.90	0.73	-287	14025.21	0.19	-322	6303.55	0.42

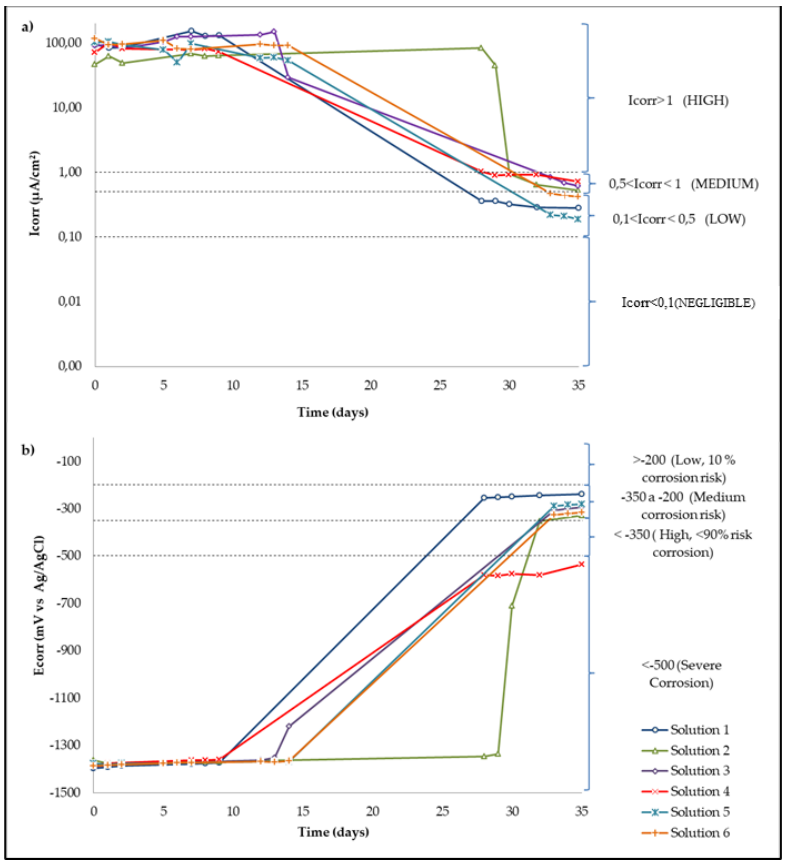

Figure 3. Evolution in time of a) I_{corr} and b) E_{corr} of the wires.

Starting points results were very electronegative in all solutions (–1.4V) and with corrosion densities around 100µA/cm². After 35 testing days, the potential increased to less electronegative values, higher than -0.3V (except for solution 4). Corrosion density decreased to 0.5µA/cm². These values of E_{corr} were also recorded in other works. In particular, for pH values of 13, Zn is actively dissolved giving rise to a soluble phase of $Zn(OH)_4^{2-}$ in the potential range between −1.35 to −1.45 VSCE [28]. Current corrosion density decreased until they reach values between 0.1 and 1µA/cm².

Solution containing only sulfate ions SO_4^{2-} (Solution 1), begins with active I_{corr} (97.24 µA/cm²) and a fairly electronegative E_{corr} (-1.4V). Initial values recorded for E_{corr} and I_{corr} indicate that galvanized layer upon contact with alkaline medium dissolves anodically with the consequent evolution of hydrogen on the galvanized surface [6, 7]. After ten testing days, these electrochemical parameters changed. Wire became covered with a passive layer and hydrogen evolution process slowed down. I_{corr} values decreased and reached 0.28µA/cm² at the end of the test. This value is within the limits representing a low corrosion state($0.1 > Icorr < 0.5\ \mu A/cm^2$). As has also been shown in other works [10, 12, 24], that a passive layer is formed over time. This layer is capable of reducing the initial corrosion density. This passive layer could be $Zn_4(SO_4)(OH)_6{\cdot}3H_2O$ (Zhu, Persson, Thierry, & Taxen, 2000) in absence of Ca^{2+} ions.

According to Acha [10] and Liu [11], 0.04M sulfate ion in saturated $Ca(OH)_2$ with a pH value of 12.4 would behave as a depassivating ion. An increase of 0.3 units of pH in

Preprints (www.preprints.org) | NOT PEER-REVIEWED | Posted: 25 April 2022 doi:10.20944/preprints202204.0223.v1

presence of sulfates is not enough for passivate the steel. Vigneshwaran *et al.* [29] considered fixed amounts of sulfate ion of 2000 and 20000ppm (0.02 and 0.2M respectively) to study the carbon steel corrosion at 12.6 and 13.3 pH values. While at pH = 12.6 steel corrodes, at a pH of 13.3 the passive layer is not destabilized. Variation of just one tenth of the pH value (12.7 *vs.* 12.6) changes the sulfate ion aggressiveness. With a sulfate ion it is passivated. The corrosion ability of sulfate ion depends on the pH and the type of steel.

When Ca^{2+} ions (solution 2) were added to sulfate solution, the initial I_{corr} value of 47.26 μA/cm² was half of I_{corr} value from solution 1 and lowest value of all solutions. This initial corrosion decreased over time. However, it does more slowly than in the rest of the solutions. Wire did not reach a moderate corrosion until 30 days of testing. The Ca^{2+} concentration was 100 times lower than the sulfate one. The initial concentration of dissolved sulfate would be decreasing half when precipitating as calcium sulfate. The passive layer on the surface of the steel in presence of calcium could be different from the previous solution and present a slowly development. Some authors[7, 8] identified a passive layer of calcium hydroxyzincate $Ca(Zn(OH)_3)_2$. They indicated the stability limit for this layer at a pH value of 13.3. Above this pH, the larger size of the crystals do not allow to cover the entire surface of the steel. The I_{corr} value at the end of the test (0.53 μA/cm²) was within the limits that represent moderate corrosion($0.5 > Icorr < 1\,\mu A/cm^2$). At studied pH, presence of Ca^{2+} coating turn out to be less protective.

The protection of the wire in presence of Ca^{2+} ions was modified when NH_4^+ ammonium ion was added to the solution (solution 3). At the beginning the I_{corr} (92.45 μA/cm²) was at least twice the solution 2 (47.26 μA/cm²) and was very similar to the sulfate solution. Higher ionic charge increased the solubility of calcium sulfate. Wire began to be covered by a passive layer after fifteen days of testing. The I_{corr} obtained after 35 days reached 0.62 μA/cm². It achieved limits that represent a state of moderate corrosion($0.5 > Icorr < 1\,\mu A/cm^2$). When bicarbonate was added (solution 4), it is observed initial I_{corr} value of 72.48 μA/cm2. Lower than the previous solution and higher than solution 2. Solubility of zinc carbonate ($1.4 \cdot 10^{-11}$) is lower than calcium sulphate ($\approx 9.1 \cdot 10^{-6}$). Therefore Zn ions could react with bicarbonate ions according to Equation 5 to give corresponding carbonates with CO_2 released [13] removing sulfate ions from the solution.

$$Zn^{2+} + HCO_3^- \leftrightarrow ZnCO_3 + H_2O + CO_2 \quad (5)$$

At the end of the test, the I_{corr} (0.73 μA/cm²) was the highest of the six solutions and it was in the limits that represent moderate corrosion with low tendency values ($0.5 > Icorr < 1\,\mu A/cm^2$). The corrosion potential shifted to more negative values (-537mV), the most electronegative of the six solutions. Passive film could be formed by hexagonal crystals of $ZnCO_3$ and monoclinic crystals of hydrozincite $Zn_5(CO_3)_2(OH)_6$. This passive layer would be the least protective.

Subsequently, initial corrosion density adding Mg^{2+} (solution 5) was 102 μA/cm². It was higher than previous solutions. After 15 days the passive layer began to form. I_{corr} values after 35 days (0.19 μA/cm²) were within the limits of low corrosion state with a negligible tendency ($Icorr < 0{,}1\,\mu A/cm^2$). This corrosion density was the lowest of all solutions, which would mean that passive layer formed under these conditions would be the most protective. These results agree with those found by Neupane *et al.* [21].They compare the dissolution effect of Na_2SO_4, NH_4SO_4 and $MgSO_4$ on galvanized steel. They found that corrosion rate in presence of NH_4^+ ion is higher than of the Mg^{2+} ion. However, if pH of the solution was not buffered, the addition of magnesium and ammonium sulfate accompanied by a decrease in the initial pH of the solution causes an increase in the corrosion rate, as shown in the study by Xu [20].

Lastly, once the behavior of the wire in chloride-free media was known, its behavior in a medium contaminated with Cl^- (solution 6) was studied. Initial value of I_{corr} was 119μA/cm², the highest of the six solutions, despite the fact that the concentration of this

Preprints (www.preprints.org) | NOT PEER-REVIEWED | Posted: 25 April 2022 doi:10.20944/preprints202204.0223.v1

ion was lower than the one with sulfate ion. I_{corr} values at 35 days (0.42 µA/cm²) were higher than the corrosion of the sulfate solution. It was within the limits of low corrosion state with a negligible tendency. Passive layer of simonkolleite $Zn_5Cl_2(OH)_8{\cdot}H_2O$ would thus be less protective than zinc hydroxysulfate, $(Zn_4(SO_4)(OH)_6{\cdot}3H_2O$.

3.2. EIS Results

As noted above, impedance measurement was useful to be able to complete the R_p calculation in the linear polarization resistance (LPR) method. In addition, it allows determining the resistance of different parts that make up a system.

One of the key aspects of the technique as a tool to research the electrical and electrochemical properties of systems is the direct relationship between real behavior of a system and that of a circuit made up of a set discrete component of electrical components, called an equivalent circuit. The most accurate circuit will be the one with the fewest possible time constants, which would provide a clear physical meaning [30]. Nyquist and Bode diagrams are obtained with their respective adjustment through the equivalent circuit to determine values of each parameter that make up the system.

Figure 4 shows the resulting example from the Nyquist and Bode diagram obtained with the adjustment through the equivalent circuit for solution 1. The equivalent circuit used in this study consisted of two constants connected in series with the resistance of the electrolyte (Figure 5). Elements of the circuit had the following physical meanings: R_s was related to the resistance of the electrolyte (solution). From the addition of bicarbonate ions (solution 4), the R_s increased due to the greater presence of solid carbonate species in the solution; the first time constants, R_c and C_c, were attributed to the resistance of faradaic charge transfer processes and their capacitance. The second time constants, R_{ct} and C_{ct}, were related to the charge transfer resistance or mass transfer resistance. The latter was comparable to that obtained by the linear polarization resistance method (Rp). Constant phase element (Q) was used instead of a pure capacitance in the adjustment because of the heterogeneity of the layer on the surface of the wire [30,31]. From the Nyquist diagram it can be seen values corresponding to the high frequency zone (1×10^5 Hz), given by the diameter of the first semicircle. It corresponds to R_c and C_c. R_{ct} and C_{ct} iwas given by the diameter of the second semicircle in the low frequency zone (0.01 Hz).

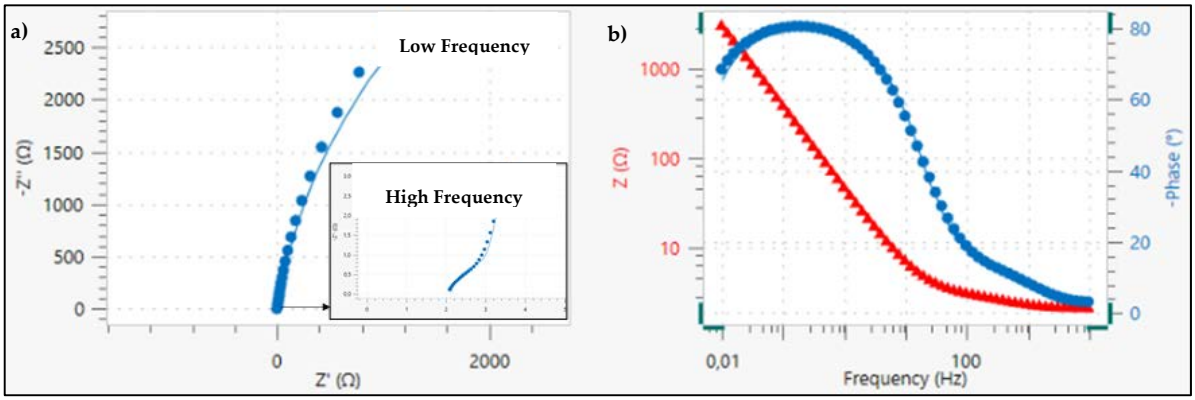

Figure 4. a) EIS results with adjustment through equivalent circuit. b) Nyquist and Bode diagram for solution 1 at day 35.

Preprints (www.preprints.org) | NOT PEER-REVIEWED | Posted: 25 April 2022 doi:10.20944/preprints202204.0223.v1

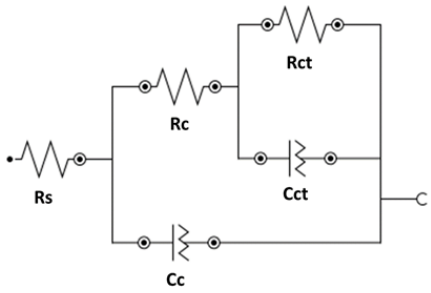

Figure 5. Equivalent circuit.

Figure 6 and Figure 7 shows the Nyquist diagram with equivalent circuit adjustment resulting from study cases after 35 days. Parameters obtained from adjustment may be observed in Table 3. From Nyquist diagrams it is possible to confirm the beginning of the formation of a passive layer on the surface of the wire. It is possible to observe the diameter of the second semicircle increasing.

Table 3. Parameters obtained through Equivalent Circuit of the Nyquist Diagram

Solution	Rs (Ω)	Rc (Ω)	Cc (F)	Rct (Ω)	CPE (F)	χ^2
1	2.11	1.55	0,00094	10169	0,00311	0.036
2	1.84	2.18	0,00045	5346	0,00042	0.024
3	2.13	2.95	0,00244	4777	0,00195	0.034
4	3.87	4.48	0,00189	4665	0,00661	0.036
5	2.93	2.87	0,00045	14923	0,00094	0.019
6	3.03	4.83	0,00157	7240	0,00123	0.016

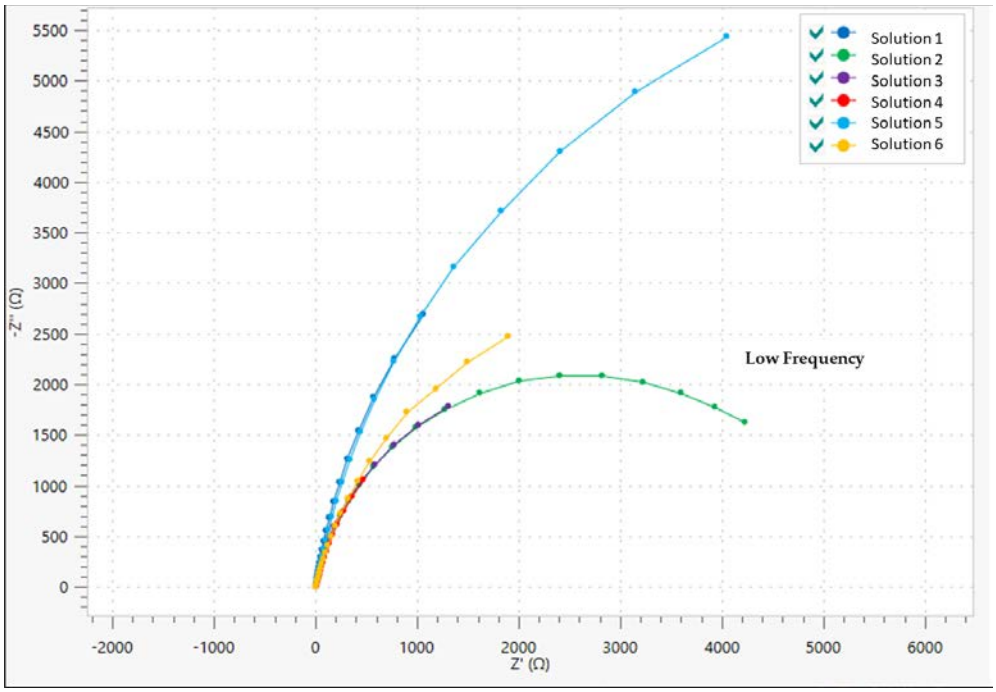

Figure 6. Nyquist diagram at Low Frequency Zone (0.01 Hz).

Preprints (www.preprints.org) | NOT PEER-REVIEWED | Posted: 25 April 2022 doi:10.20944/preprints202204.0223.v1

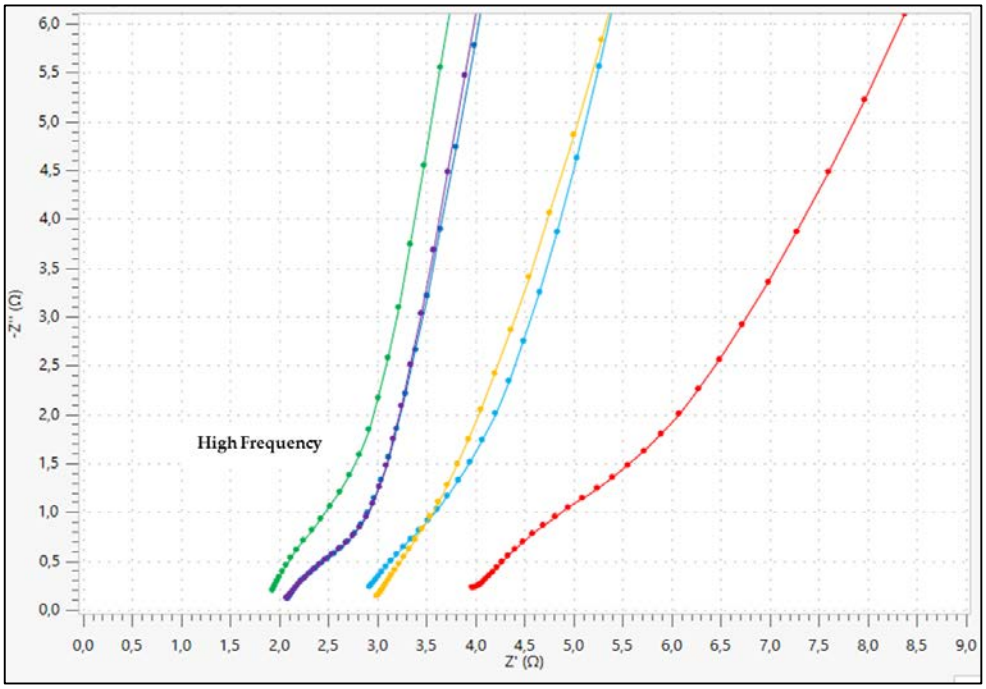

Figure 7. Nyquist diagram at High Frequency Zone ($1 \cdot 10^5$ Hz).

Equivalent circuit used seems to be the correct one because it has the fewest possible time constants with clear physical meaning. The deviation (X^2) in all cases is less than 0.03. Charge transfer resistance on the wire surface (R_{ct}) is compared (Table 4) with the obtained R_p through linear polarization resistance to validate the results obtained through EIS. The equivalence is maintained in all cases except for solution 4. The percentage difference between both methods is less than 14%. Although the difference with solution 4 is 24%. Its magnitudes are equal, which represents a state of medium corrosion in both cases ($0.5 > I_{corr} < 1\ \mu A/cm^2$). Differences are valid and are mainly attributed to the fact that LPR uses direct current while EIS technique uses alternating current (sinusoidal disturbance of electric potential of variable frequency to the studied material). Order of passive layer stability is confirmed by the two electrochemical techniques (solution 5 < solution 1 < solution 6 < solution 2 > solution 3 > solution 4).

Table 4. *Rp* obtained by LPR and EIS.

Solution	Rp (LPR) (Ω)	Rct (EIS) (Ω)	Difference (%)
1	9383	10169	8
2	5040	5346	6
3	4306	4777	10
4	3661	4665	24
5	14025	14923	6
6	6304	7240	14

3.3. Morphology of steel surface

Figure 8 shows different steels surfaces images obtained by optical microscopy and SEM after electrochemical analysis in synthetic solutions. No traces of iron oxides are observed on the surface of the wires. Solution 1 wire is homogeneously coated with pris-

Preprints (www.preprints.org) | NOT PEER-REVIEWED | Posted: 25 April 2022 doi:10.20944/preprints202204.0223.v1

matic crystals possibly of $Zn_4(SO_4)(OH)_6 \cdot 3H_2O$. Solution 3 wire shows oxide layer distributed leaving large voids on the surface. Size and coating of the crystals in the rest of the wires varies. It can be attributed to insoluble crystalline products such as $Zn_5(CO_3)_2(OH)_6$, $ZnCO_3$, $Zn_5Cl_2(OH)_8 \cdot H_2O$, ZnO, or others with ability to passivate galvanized steel to a greater or lesser extent [15]. Some areas of exposure are darker in color due to increased detachment of the zinc layer and oxidation of the steel.

Only an isolated white crystal of calcium hydroxyzincate $Ca(Zn(OH)_3)_2$ was found on the surface of the wire exposed to solution 2. Due to the high pH of the solution, crystal becomes larger and does not have the capacity to homogeneously coat the surface of the wire (Figure 9) [14]. By observing SEM appearance of this crystal, it was possible to identify a totally different morphology from ones observed on the surface of the other wires. Small crystallized threads are observed.

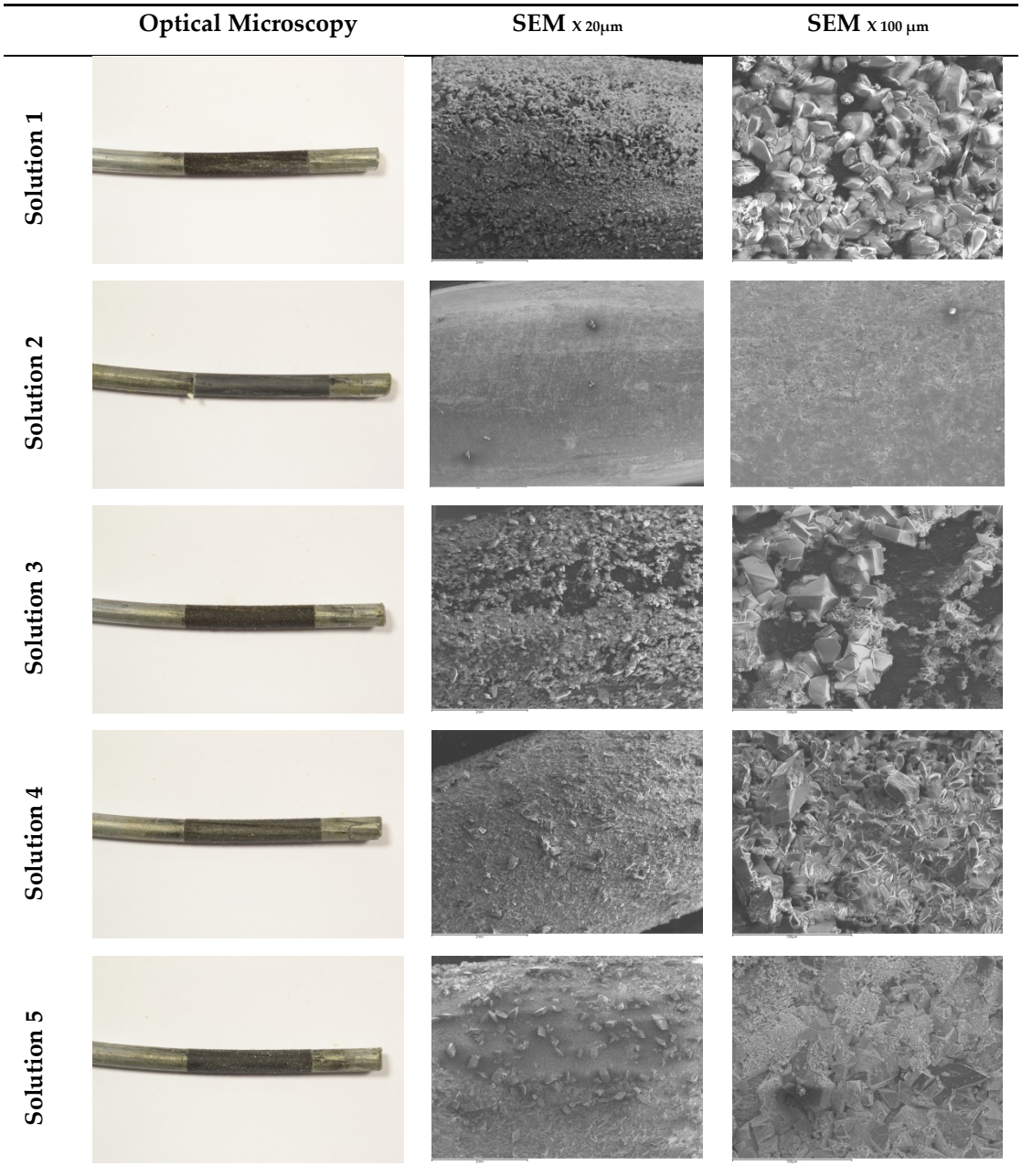

Preprints (www.preprints.org) | NOT PEER-REVIEWED | Posted: 25 April 2022 doi:10.20944/preprints202204.0223.v1

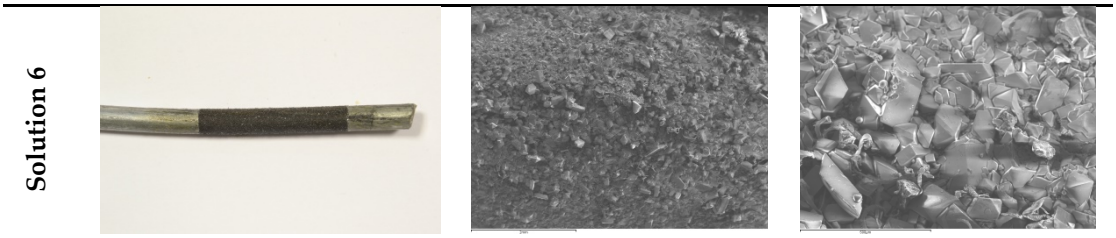

Figure 8. Optical microscopy and SEM results of the steel surfaces.

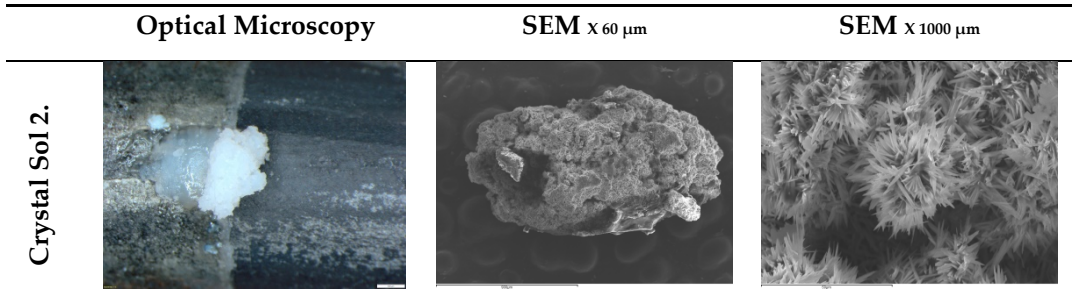

Figure 9. Optical microscopy and SEM crystal results $Ca(Zn(OH)_3)_2$ solution 2.

4. Conclusions

Galvanized steel in contact with a strongly alkaline solution (pH = 12.7) and in presence of sulfates, dissolves anodically with corrosion potentials around –1.4V and corrosion densities around 100μA/cm². Over time, the surface of the steel is covered with a protective layer and the corrosion potential increases until reaching values of -0.25V in correspondence with a decrease in corrosion density to 0.3μA/cm², greater than 0.1 μA/cm² at any case. Consequently, the presence of sulfate ions is capable of depassivating galvanized steel at highly alkaline pH.

The presence of other anions and cations together with the sulfate ions keeps the corrosion process active. Nature of the passive layer depends on the present ions. Cations and anions studied contribute to the increase in the corrosion density of the sulfate ions. The magnitude of this increase follows the following order: $NH_4^+ > Ca^{2+} > Mg^{2+}$ and $HCO_3^- > Cl^- > SO_4^{2-}$.

At a pH of 12.7, the hydroxyzincate crystal formed on the surface of the steel immersed in the solution of sulfate and calcium ions is large and occurs in isolation without the ability to cover the entire surface of the steel.

Author Contributions: Conceptualization, A.B. and A.M.; methodology, A.B, C.A, A.M. and J.G.; software, A.B.; validation, A.B., C.A. and A.M.; formal analysis, A.B and C.A.; investigation, A.B. and C.A.; resources, A.B. and C.A.; data curation, C,A.; writing—original draft preparation, A.B. and C,A; writing—review and editing, A.B., C.A ,A.M and J.G.; visualization, A.M.; supervision, A.M. and J.G.; project administration, A.M and J.G.

Funding: This research was funded by the Ministry of Economy and Competitiveness of Spain by means of the Research Fund Projects RTI2018-100962-B-100 and PID2019-108978RB-C31R.

Conflicts of Interest: Authors declare no conflict of interest.

References

1. Powers, R.W.; Breiter, M.W. The Anodic Dissolution and Passivation of Zinc in Concentrated Potassium Hydroxide Solutions. *J. Electrochem. Soc.* **1969**, *116*, 719, doi:10.1149/1.2412040.
2. *Electrochemistry*; 1974; Vol. 4; ISBN 978-0-85186-037-4.
3. Muralidharan, V.S.; Rajagopalan, K.S. Kinetics and Mechanism of Passivation of Zinc in Dilute Sodium Hydroxide Solutions. *Br. Corros. J.* **1979**, *14*, 231–234, doi:10.1179/000705979798358607.

4. Riecke, E., Investigations on the influence of zinc on the corrosion behavior of high strength steels, Mater. Corros. 30 (1979) 619-631
5. Parsons, R. Atlas of Electrochemical Equilibria in Aqueous Solutions. *J. Electroanal. Chem. Interfacial Electrochem.* **1967**, *13*, 471, doi:10.1016/0022-0728(67)80059-7.
6. Recio, F.; Alonso, C.; Gaillet, L.; Sánchez Moreno, M. Hydrogen Embrittlement Risk of High Strength Galvanized Steel in Contact with Alkaline Media. *Corros. Sci. - CORROS SCI* **2011**, *53*, 2853–2860, doi:10.1016/j.corsci.2011.05.023.
7. Macías, A.; Andrade, C. Corrosion Rate of Galvanized Steel Immersed in Saturated Solutions of $Ca(OH)_2$ in the PH Range 12-13.8. *Br. Corros. J.* **1983**, doi:10.1179/bcj.1983.18.2.82.
8. Blanco, M.T.; Andrade, C.; Macías, A. Estudio Por SEM de Los Productos de Corrosión de Armaduras Galvanizadas Sumergidas En Disoluciones de PH Comprendido Entre 12,6 y 13,6. *Mater. Constr.* **1984**, *34*, 55–66, doi:10.3989/mc.1984.v34.i195.946.
9. Macías, A.; Andrade, C. Corrosion of Galvanized Steel in Dilute $Ca(OH)_2$ Solutions (PH 11.1–12.6). *Br. Corros. J.* **1987**, *22*, 162–171, doi:10.1179/000705987798271505.
10. Corrosión bajo tensión de alambres de acero pretensado en medios neutros con HCO_3^- y alcalinos con SO_4^{2-}. 321.
11. Liu, G.; Zhang, Y.; Ni, Z.; Huang, R. Corrosion Behavior of Steel Submitted to Chloride and Sulphate Ions in Simulated Concrete Pore Solution. *Constr. Build. Mater.* **2016**, *115*, 1–5, doi:10.1016/j.conbuildmat.2016.03.213.
12. Bertolini, L.; Carsana, M. High PH Corrosion of Prestressing Steel in Segregated Grout. In Proceedings of the Modelling of Corroding Concrete Structures; Andrade, C., Mancini, G., Eds.; Springer Netherlands: Dordrecht, 2011; pp. 147–158.
13. Roventi, G.; Bellezze, T.; Barbaresi, E.; Fratesi, R. Effect of Carbonation Process on the Passivating Products of Zinc in Ca(OH)2 Saturated Solution. *Mater. Corros.* **2013**, *64*, 1007–1014, doi:10.1002/maco.201206868.
14. Farina, S.B.; Duffó, G.S. Corrosion of Zinc in Simulated Carbonated Concrete Pore Solutions. *Electrochimica Acta* **2007**, *52*, 5131–5139, doi:10.1016/j.electacta.2007.01.014.
15. Zhu, F.; Persson, D.; Thierry, D.; Taxén, C. Formation of Corrosion Products on Open and Confined Zinc Surfaces Exposed to Periodic Wet/Dry Conditions. *Corrosion* **2000**, *56*, 1256–1265, doi:10.5006/1.3280514.
16. Ramirez, E.; González, J.A.; Bautista, A. The Protective Efficiency of Galvanizing against Corrosion of Steel in Mortar and in Ca(OH)2 Saturated Solutions Containing Chlorides. *Cem. Concr. Res.* **1996**, *26*, 1525–1536, doi:10.1016/0008-8846(96)00150-0.
17. Yadav, A.; Nishikata, A.; Tsuru, T. Degradation Mechanism of Galvanized Steel in Wet–Dry Cyclic Environment Containing Chloride Ions. *Corros. Sci.* **2004**, *46*, 361–376, doi:10.1016/S0010-938X(03)00153-7.
18. Liu, S.; Sun, H.; Sun, L.; Fan, H. Effects of PH and Cl− Concentration on Corrosion Behavior of the Galvanized Steel in Simulated Rust Layer Solution. *Corros. Sci.* **2012**, *65*, 520–527, doi:10.1016/j.corsci.2012.08.056.
19. Persson, D.; Thierry, D.; Karlsson, O. Corrosion and Corrosion Products of Hot Dipped Galvanized Steel during Long Term Atmospheric Exposure at Different Sites World-Wide. *Corros. Sci.* **2017**, *126*, doi:10.1016/j.corsci.2017.06.025.
20. Xu, P.; Jiang, L.; Guo, M.-Z.; Zha, J.; Chen, L.; Chen, C.; Xu, N. Influence of Sulfate Salt Type on Passive Film of Steel in Simulated Concrete Pore Solution. *Constr. Build. Mater.* **2019**, *223*, 352–359, doi:10.1016/j.conbuildmat.2019.06.209.
21. Neupane, S.; Hastuty, S.; Yadav, N.; Singh, N.; Gupta, D.K.; Yadav, B.; Singh, S.; Karki, N.; Kumari Das, A.; Subedi, V.; et al. Effects of NH4 +, Na+, and Mg2+ Ions on the Corrosion Behavior of Galvanized Steel in Wet–Dry Cyclic Conditions. *Mater. Corros.* **2021**, *72*, 1388–1395, doi:10.1002/maco.202112360.
22. metálicos, A. 112 C. y protección de los materiales *Norma Española UNE 112072*; 2011;
23. Denny Jones *Principles and Prevention of Corrosion*; 1996;
24. Andrade, C.; Alonso, C. Corrosion Rate Monitoring in the Laboratory and On-Site. *Constr. Build. Mater.* **1996**, *10*, 315–328, doi:10.1016/0950-0618(95)00044-5.

25. Andrade, C.; Castelo, V.; Alonso, C.; González, J.A. The Determination of the Corrosion Rate of Steel Embedded in Concrete by the Polarization Resistance and AC Impedance Methods. *Corros. Eff. Stray Curr. Tech. Eval. Corros. Rebars Concr.* **1986**, doi:10.1520/STP18302S.
26. González, J.A.; Albéniz, J.; Feliu, S. Valores de la constante *B* del método de resistencia de polarización para veinte sistemas metal-medio diferentes. *Rev. Metal.* **1996**, *32*, 10–17, doi:10.3989/revmetalm.1996.v32.i1.926.
27. Hladky, K.; Callow, L.M.; Dawson, J.L. Corrosion Rates from Impedance Measurements: An Introduction. *Br. Corros. J.* **1980**, *15*, 20–25, doi:10.1179/000705980798318627.
28. Bonk, S.; Wicinski, M.; Hassel, A.W.; Stratmann, M. Electrochemical Characterizations of Precipitates Formed on Zinc in Alkaline Sulphate Solution with Increasing PH Values. *Electrochem. Commun. - ELECTROCHEM COMMUN* **2004**, *6*, 800–804, doi:10.1016/j.elecom.2004.05.012.
29. Krishna Vigneshwaran, K.K.; Permeh, S.; Echeverría, M.; Lau, K.; Lasa, I. Corrosion of Post-Tensioned Tendons with Deficient Grout, Part 1: Electrochemical Behavior of Steel in Alkaline Sulfate Solutions. *Corrosion* **2017**, *74*, 362–371, doi:10.5006/2541.
30. Hu, J.; Koleva, D.; Petrov, P.; Breugel, K. Polymeric Vesicles for Corrosion Control in Reinforced Mortar: Electrochemical Behavior, Steel Surface Analysis and Bulk Matrix Properties. *Corros. Sci.* **2012**, *65*, 414–430, doi:10.1016/j.corsci.2012.08.043.
31. Garces, P.; Andrade, M.; Saez, A.; Alonso, C. Corrosion of Reinforcing Steel in Neutral and Acid Solutions Simulating the Electrolytic Environments in the Micropores of Concrete in the Propagation Period. *Corros. Sci. - CORROS SCI* **2005**, *47*, 289–306, doi:10.1016/j.corsci.2004.06.004.